Solar Energy Materials & Solar Cells 105 (2012) 119–124

Contents lists available at SciVerse ScienceDirect

Solar Energy Materials & Solar Cells

journal homepage: www.elsevier.com/locate/solmat

Self-assembled Cu(In,Ga)Se_2 nanocrystals formed by Ar ion beam irradiation

Ji-Yeong Lee [a,b], Sk.Faruque Ahmed [b], Min-Ho Park [c], Seung-kyu Ha [b], Jong-Ku Park [b], Jae Ho Yun [d], Se Jin Ahn [d], Kwang-Ryeol Lee [b], Won Jun Choi [b], Myoung-Woon Moon [b,*], Cheol-Woong Yang [a,c,**]

[a] Department of Nanoscience and Nanotechnology, Center for Nanotubes and Nanostructured Composites, Sungkyunkwan University, Suwon 440-746, Republic of Korea
[b] Future Convergence Technology Research Division, Korea Institute of Science and Technology, 39-1, Sangwolgok, Seongbuk, Seoul 130-650, Republic of Korea
[c] School of Advanced Materials Science and Engineering, Sungkyunkwan University, Suwon 440-746, Republic of Korea
[d] Solar Cells Research Center, Korea Institute of Energy Research, Daejeon 305-343, Republic of Korea

ARTICLE INFO

Article history:
Received 2 May 2011
Received in revised form
15 February 2012
Accepted 27 May 2012

Keywords:
Ion beam irradiation
CIGS
Nano-dot
Nanocrystals
Photovoltaic system

ABSTRACT

We developed a simple and effective method for the large scale formation of self-assembled Cu(In,Ga)Se_2 (CIGS) nanocrystals by ion beam irradiation. The compositional changes and morphological evolution were observed as a function of the irradiation time. As the ion irradiation time increased, the nano-dots were transformed into a nano-ridge structure due to the competition between sputtering and diffusion processes during irradiation. In terms of the stoichiometry of the CIGS nano-dots, an increase in the Cu content was observed while the Se content decreased. The PL peak of the nano-dots formed CIGS thin film exhibited a blue-shift. Uniformly formed crystalline CIGS nano-dots can be adopted to increase the p–n junction area and the size confinement effect between the CdS and CIGS film in solar cell systems. This simple method can be exploited for band-gap engineering and enhancing photovoltaic properties.

1. Introduction

Many different materials such as amorphous silicon and polycrystalline chalcopyrite materials of Cu(In,Ga)Se_2 (CIGS) have been employed in thin film photovoltaic systems. In particular, CIGS-based solar cells have advantages of low cost, long-term stability, a high absorption coefficient with a thin layer, and applicability to stiff or flexible substrates [1–3]. Thin film solar cells comprised of CIGS have achieved remarkable conversion efficiencies as high as 20.3% [4]. However, there is still opportunity to increase the cell efficiency. More recently, solar cells based on nanowires or nanocrystals (NCs) have attracted much attention as a promising structure due to their properties including single crystallinity, size confinement, and increased surface to volume ratio. In addition, an array of CIGS NCs often possesses superior optical absorption due to their light-scattering and trapping morphologies. There have been a number of reports on the synthesis of $CuInSe_2$ NCs using various methods. Qian et al. [5,6] synthesized $CuInSe_2$ nanoparticles, nanowhiskers, and nanorods *via* solvothermal reactions of Cu, In, and Ga salts/elements with selenium powders in ethylenediamine. Guo et al. [7] and Koo et al. [8] prepared $CuInSe_2$ nanorings with a hexagonal shape and NCs with a trigonal pyramidal shape using oleylamine as a solvent. Peng et al. [9] reported the synthesis of In_2Se_3 and $CuInSe_2$ nanowires by VLS techniques. Huang et al. [10,11] also reported the CIGS quantum dots on an ITO substrate by magnetron sputtering. In addition, an individual $CuInSe_2$ nanowire has also been synthesized from a solid-state reaction between an In_2Se_3 nanowire and contacting copper pads [12]. Large scale synthesis of CuSe, $CuInSe_2$ nanowire was also reported by Xu et al. [13]. However, to the best of our knowledge, there have not been reports on the formation of CIGS NCs directly on the surface of a CIGS thin film to date. In addition, the optical properties can be tuned by tailoring the size and shape of the NCs due to quantum confinement effects on the CIGS surface layer where the electrical junction forms in photovoltaic devices [14]. In this work, we developed a simple and effective method for the formation of self-assembled CIGS NCs by ion beam irradiation on the large scale to increase the p–n junction area from the CIGS/CdS interface. The crystal structure and chemical composition changes of the CIGS NCs were characterized by nano-beam electron diffraction (NBED) measurements and scanning transmission electron microscopy (STEM)/energy dispersive X-ray spectrometry (EDS). The band-gap energies of the CIGS thin films with and without NCs were measured using low temperature photoluminescence (PL).

2. Experimental details

The CIGS thin films were grown by a three-stage process involving the co-evaporation of elemental Cu, In, Ga, and Se on

* Corresponding author. Tel.: +82 2 958 5487; fax: +82 2 958 5509.
** Corresponding author. Tel.: +82 31 290 7362; fax: +82 31 290 7410.
E-mail addresses: mwmoon@kist.re.kr (M.-W. Moon), cwyang@skku.edu (C.-W. Yang).

0927-0248/$ - see front matter © 2012 Elsevier B.V. All rights reserved.
http://dx.doi.org/10.1016/j.solmat.2012.05.034

molybdenum-deposited soda lime glass. The details of the growth process and the growth conditions have been reported elsewhere [15]. For the Ar ion beam irradiation, the as-grown samples were transferred into a chamber with a broad ion beam system with linear end hall type ion gun and the chamber was evacuated to a base pressure of 2×10^{-5} mbar. The flow rate of Ar gas was 8 sccm and the anode voltage of the ion gun was fixed at 1.0 kV during irradiation. The distance between the ion source and the substrate holder was about 15 cm. A radio frequency (RF) bias voltage of -600 V was applied to the substrate holder and the irradiation time was varied from 1 to 10 min. By considering the current density and irradiation area of the sample, Ar ion beam irradiation for 1 min is equivalent to an ion fluence of 1.91×10^{16} ions/cm^2. The macro-structural analysis was conducted using X-ray diffraction (XRD) (Panalytical X'pert Highscore) with Cu Kα X-rays.

The surface morphology of the CIGS thin films was explored using a field-emission scanning electron microscope as part of a dual-beam focused ion beam (FIB) system (Nova 600, FEI). The cross-sectional specimens examined by the transmission electron microscopy (TEM) were prepared by using the FIB. The microstructure and chemical composition of the samples were analyzed by a high-resolution TEM (JEM-2100F, JEOL) operating at 200 kV combined with scanning transmission electron microscopy (STEM)/energy dispersive X-ray spectrometry (EDS). Nano-beam electron diffraction (NBED) and selected area-diffraction (SAD) experiments were employed to determine the crystallographic phases of the nanocrystals formed on the CIGS films. The optical band-gap was measured by using low-temperature PL (photoluminescence) at an average temperature of 15 K with a diode-pumped (7 mW power) solid state (DPSS) continuous-wave laser operating at 532 nm (SDL-532-300T) and a monochromator (SpectraPro 2300i). Prior to the PL measurements of the ion beam-treated CIGS surfaces, a bare CIGS substrate was tested for its PL emission to determine any fluorescence effects arising from the glass substrate. No fluorescence was detected in the wavelength range that was used for the analysis of the PL peaks of the CIGS thin films.

3. Results and discussion

The grain sizes of the pristine CIGS film grown by the co-evaporation method ranged from 1.5 to 2.3 μm and the film thickness was 2.1 μm, as shown in Fig. 1(a). Fig. 1(b)–(e) display top-view and tilted-view (insets) images revealing the morphologies of the nanostructures formed on the surface as a function of the Ar ion beam irradiation time. A normal incidence and a constant anode voltage of 1 kV were employed for these samples. The average size of the nano-dots was measured to be approximately 23 nm for the 1 min treated sample in Fig. 1(b). No noticeable change in the dot configuration was observed below an irradiation time of 1 min, irrespective of the acceleration voltage. As the acceleration voltage was increased at a given treatment time, the size of nano-dots became larger without any noticeable change in their shape. The smallest nano-dots were about 9 nm after 1 min of treatment. Increasing the irradiation time resulted in a morphological change of the NCs. Nano-dots coexisted with a nano-ridge structure up to an irradiation time of 5 min. As the irradiation time increased, the shape of the nano-dots became elongated and the dots were transformed into nano-ridge structures with a sharp etched top on the ridge with a longer length, as shown in the insets of Fig. 1(d) and (e). XRD spectra were measured to investigate the property change of CIGS thin film before and after ion beam irradiation. Neither the peak shift nor the new phase was induced by an ion beam irradiation as shown in Fig. 1(f).

In order to understand the formation mechanism of the nanostructures, an in-depth investigation of the crystallographic and elemental changes caused by Ar ion beam irradiation was conducted using analytical TEM/STEM. The cross-sectional TEM image of the ion beam treated specimen is shown in Fig. 2(a). The position [x] marks the nano-dot on the surface of CIGS film coated by an epoxy resin to protect the surface from any possible damage during the FIB sample preparation and the [y] mark represents the inside of the CIGS film. The diameter of a nano-dot is about 23 nm as a single crystalline, as shown in Fig. 2(b) along with a height of less than 13 nm. Clear lattice fringes were observed from the high resolution TEM image of a hemispheric nano-dot, even though the surface layer was irradiated by the ion beam. Normally, ion beam irradiation results in amorphization of the target being bombarded. However, the CIGS surface layer including the nano-dot is crystalline. Therefore, in terms of the crystallinity, the surface properties were not considerably affected by the ion beam irradiation. Indexed-NBED patterns were analyzed for the [0 $\bar{2}$ 1], [1 1 0], and [2 2 1] zone axes in Fig. 2(c)–(e), respectively. The angles between the [1 1 0] and [2 2 1] zone axes and between the [1 1 0] and [0 $\bar{2}$ 1] zone axes were measured to be 36° and 60.8°, respectively. This result confirms the crystallographic system of the nano-dots to be tetragonal, which is the same as the pristine CIGS thin film.

Fig. 2(f) is the STEM/EDS result for the NCs as a function of the Ar ion beam irradiation time. The STEM/EDS analysis confirmed that the chemical composition of the pristine CIGS film labeled [y] in Fig. 2(f) was measured to be Cu (27.45 ± 2.10 at%), In (21.71 ± 2.3 at%), Ga (6.23 ± 1.34 at%), and Se (44.54 ± 2.63 at%). The chemical composition of NCs formed after 1 min and 5 min treatment changed slightly to Cu (34.48 ± 1.52 at% and 34.54 ± 3.04 at%) and Se (38.99 ± 3.05 at% and 38.77 ± 3.84 at%). However, there remained no binary Cu_xSe phase as the quaternary phase, CIGS NCs.

As shown in the line profile of the four elements in the sample treated for 1 min at 1 kV in Fig. 2(g), the most noticeable changes in the composition occurred at the near surface region down to about 35 nm from the surface (including the nano-dot indicated by [x]). This result is attributed to the penetration power of the Ar ion beam at 1 kV. Deviation from the original composition of the pristine CIGS film became greater with the 10 min treated sample. The fractions of Cu and Se were about 38.24 ± 2.64 at% and 36.55 ± 1.74 at%, respectively. However, the contents of In and Ga before and after irradiation remained the same. The amount of the increase of the Cu fraction is similar to the decrease of the Se fraction. In polycrystalline CIGS, a Cu/(In+Ga) ratio greater than 1 generally produces Cu-rich precipitates. It is believed that in Cu-rich films Cu-on-In antisite (Cu_{In}) and In vacancy (V_{In}) defects can be also formed to partially account for the deviation from compositional stoichiometry [16].

The formation mechanism of CIGS NCs can be understood by tracing their morphological evolution and elemental redistribution as a function of the irradiation time. The formation mechanism relies on a natural self-organization mechanism that occurs during the erosion of surfaces, which is based on the interplay between roughening induced by ion sputtering and smoothing due to surface diffusion. The formation kinetics is determined by etching instead of growth. Facsko et al. [17] reported that a formation process for dots is based on a surface instability induced by ion sputtering. It was found that the diameter or wavelength of dots showed no dependency on ion current density in the range of $1–4\times10^{15}$ cm^{-2} s^{-1} and also no dependency on sample temperatures controlled between -60 °C and $+60$ °C by water cooling at an ion energy of 75 to 1800 eV. In these

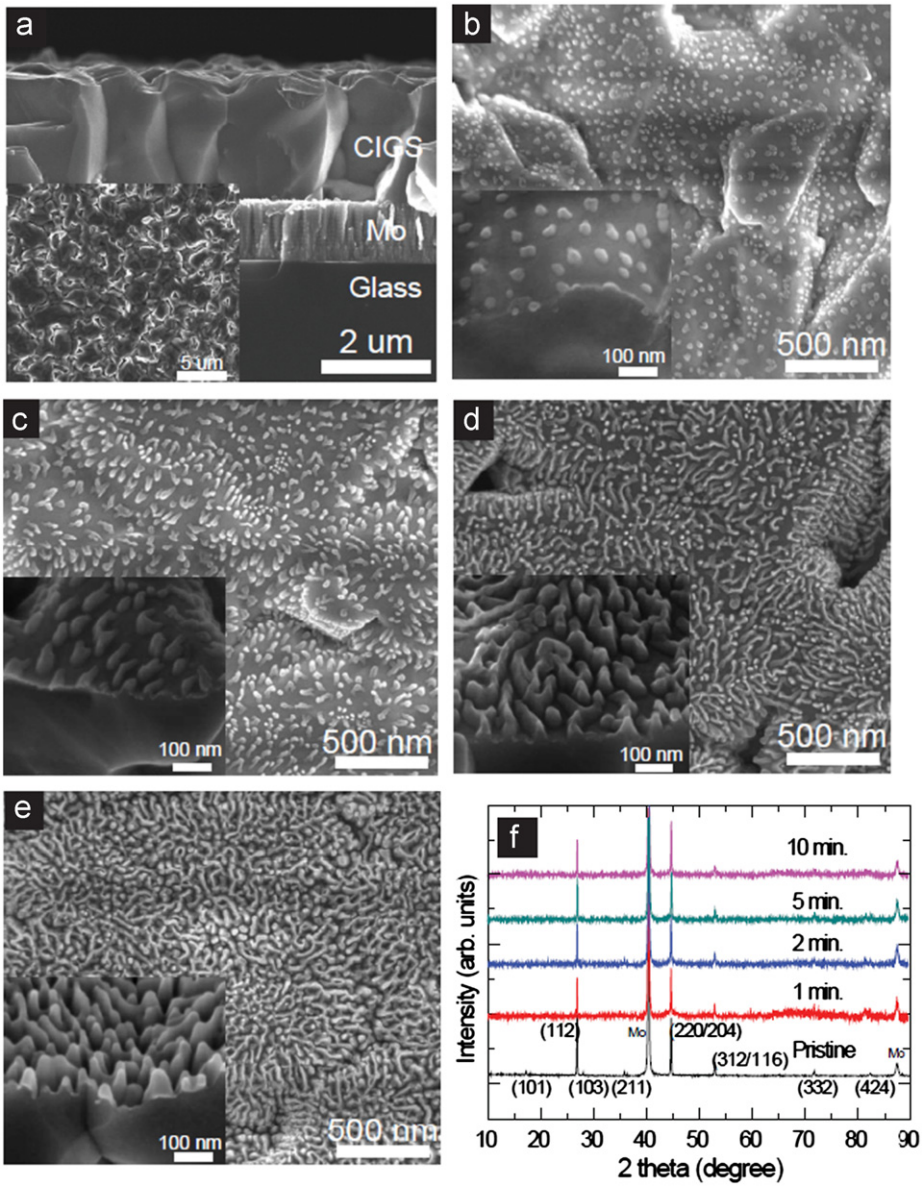

Fig. 1. (a) Cross-sectional view of a pristine CIGS film (inset is a top view). After Ar ion beam irradiation for (b) 1 min, (c) 2 min, (d) 5 min, and (e) 10 min with normal incidence at an anode voltage of 1 kV, changes in surface morphologies of the CIGS thin films occurred. The images in the insets are tilted at an angle of 52° to help illustrate the 3 dimensional shapes. (f) X-ray diffraction (XRD) spectra of CIGS films before and after Ar ion beam irradiation with different duration.

conditions, the assumption that the effective ion-induced diffusion dominates over thermal diffusion can be valid for the dot formation process. Since our experimental condition of nano-dot formation process is in the range of ion current density of 0.32×10^{15} cm^{-2} s^{-1} at an ion energy of 600 eV, which is within the effective ion-induced diffusion regime, there would be minimum temperature dependence for forming the CIGS nano-dots.

As the ion beam irradiation duration increases, shape transition occurs from uniform circular to unordered elongated configuration. The nano-dots appear in the early stage in the nonlinear regime as given by the solution of the Kuramoto–Sivashinsky (KS) equation, but for longer duration of ion beam irradiation, the surface contour evolves towards unordered patterns and enters the regime of kinetic roughening. Thus, in shorter irradiation, the dots have a circular and uniform shape and are ordered in an array with a narrow distribution. However, at longer duration, the shape of the dots becomes asymmetric with a large distribution. This stage may indicate that the process enters the kinetic roughening regime for longer sputtering [18,19]. In the case of alloy surfaces, the differences in the sputter yields and surface diffusivities of the alloy components lead to spontaneous modulations of the composition [20].

Fig. 1 shows the shape transition during ion beam irradiation on the CIGS film. At the first stage of ion beam irradiation, nano-dots are developed on the surface. Then dots merge with neighboring dots and become a nano-ridge structure. The mechanism of CIGS nano-dot formation can be attributed to the preferential sputtering of Se and clustering of the remaining elements on the surface. The CIGS NCs formation is likely to occur at a relatively faster sputtering rate for Se (5.16) when compared to Cu (1.751), In (2.135), and Ga (1.573) [21]. A relatively faster diffusivity for Cu in the alloy surfaces is also responsible for the compositional change in the CIGS NCs. Studies of copper diffusion in semiconductors, particularly in $CuInSe_2$, have demonstrated its high diffusivity [22,23]. In a CIGS or CIS system, the reported diffusion coefficients are 10^{-6}–10^{-7} cm^2/s for Cu at 200–300 °C [24], 3×10^{-13} cm^2/s for In at 400–600 °C [25], 10^{-11} cm^2/s for In and Ga at 700 °C [24,25], and 2×10^{-13} cm^2/s for Se at 700 °C [26]. The values of the diffusion

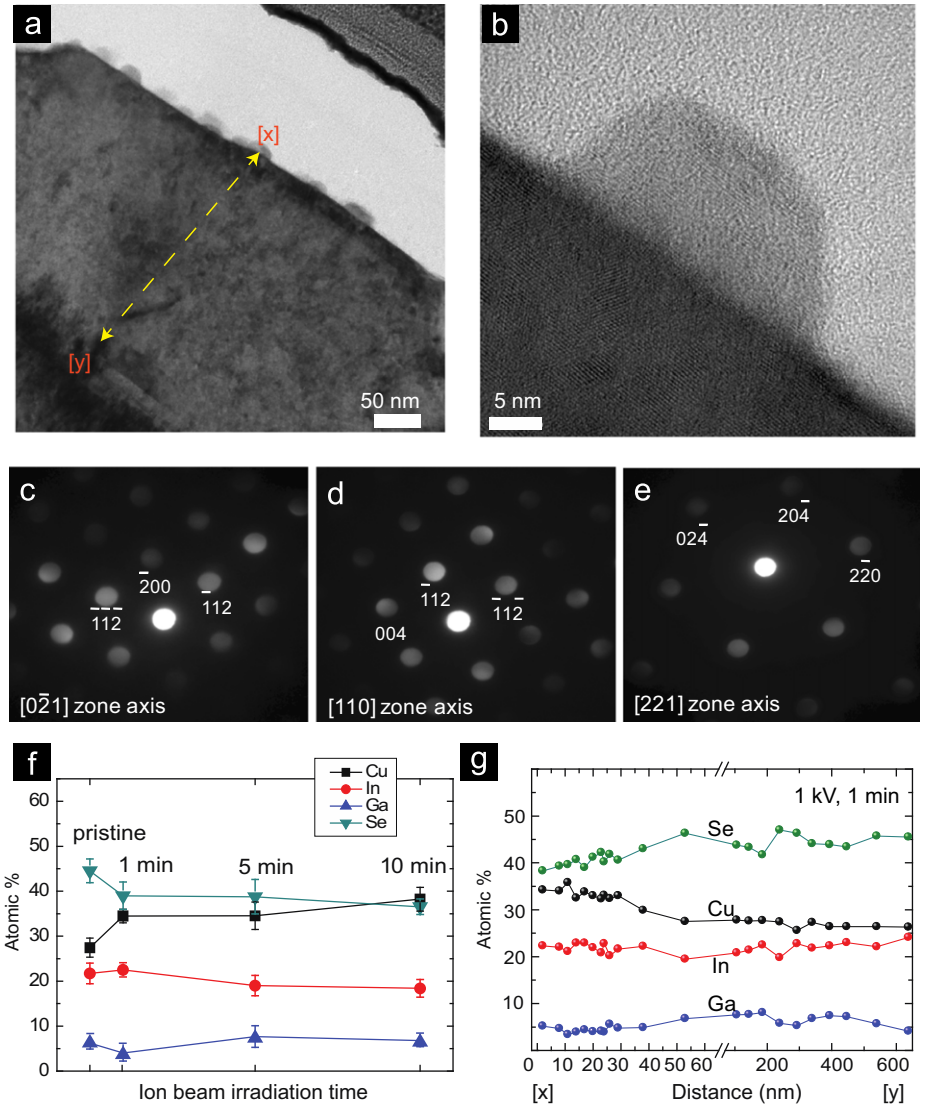

Fig. 2. (a) A low magnification image of a sample prepared by FIB (b) cross-sectional high resolution TEM image of a nano-dot formed on the surface of a CIGS thin film. The NBED patterns of a CIGS nano-dot at different zone axes are shown in (c)–(e). (f) STEM/EDS data before and after Ar ion beam irradiation as a function of treatment time. (g) The elemental distribution along the line from [x] to [y] as indicated in (a).

coefficients increase as the temperature increases. An increase in the fraction of Cu is the result of the faster diffusivity of the Cu compared to the other components. A decrease in the Se content is mainly caused by the sputtering actions of the ion beam with respect to the ion irradiation time, or equivalently, the ion fluence. This would cause the etched configuration shown in Fig. 1(c). The Cu-enriched dots can coarsen through self-assembly and easily coalesce with neighboring dots due to the relatively fast diffusivity of Cu. The dots become elongated and evolve into nano-ridge structures, as shown in the Fig. 1(b)–(e). Uniformly formed crystalline CIGS nano-dots with a slightly changed composition can lead to increase in the p–n junction area between the CdS and CIGS film and the size confinement effect with an increased surface to volume ratio.

There are reports that, due to the quantum confinement effects on the absorption spectra of quantum dots, with reduced size, the spectra shift to a higher energy [27,28]. Therefore, the size and shape of nanostructures are closely related to the change in the band-gap. And also the PL intensity has a close relationship with the morphology of the thin film. Yang et al. [29] studied with different morphologies such as nanoparticles, nanospheres, nanorods, nanoflowers, and nanorod arrays. The uniformity of the nanostructures plays a key role on the PL intensities. In this report, we measured the PL spectra by forming the various NCs on the surface of the CIGS film. The normalized PL spectra in Fig. 3 were obtained at a temperature of 15 K and a pump power of 7 mW. The pristine CIGS film exhibited a dominant near-band-edge (NBE) PL peak at 1.05 eV together with weak PL peaks at 1.15 eV (marked with an arrow) as shown in the inset of Fig. 3. Asymmetric PL peaks were consistently found at 1.05 eV at 5 different positions. The weak PL peaks at 1.15 eV have been commonly observed for the defect related peak of the CIGS film [30,31]. After Ar ion beam treatment, the PL spectrum became more asymmetric with a steep high-energy slope and gentle low-energy slope. The full-width at half-maximum (FWHM) of the PL peaks became narrower and the PL intensity became stronger by about 1 order of magnitude compared to those of the pristine CIGS film. A notable effect of the size distribution of a pattern on the PL spectrum of semiconductor materials is peak broadening or narrowing [32]. Therefore, uniformly formed NCs on the surface of the CIGS film can be responsible for the narrow and high intensity of PL spectrum.

The phonon energy of the 1 min treated samples with nano-dots was blue-shifted to 1.16 eV. As the irradiation time was

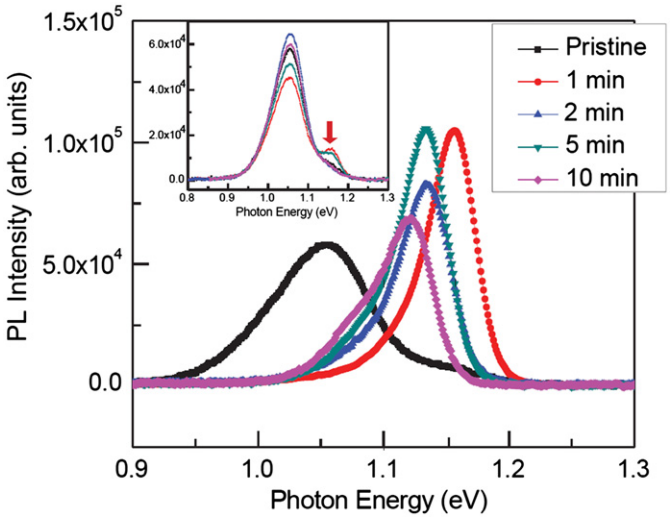

Fig. 3. Low-temperature PL spectra of NCs formed on a CIGS thin film as a function of the Ar ion irradiation time at a constant pump power of 7 mW and a temperature of 15 K. The inset shows the PL spectra of a pristine CIGS thin film obtained at five different positions. The arrows indicated the shoulder peak position.

increased from 2 min to 10 min, however, a nano-ridge structure was developed on the CIGS film and the photon energy decreased again from 1.14 to 1.12 eV of the band-gap energy. Since PL measurement is known to be a very sensitive technique, it is not surprising that the size confinement effect was measured due to the presence of CIGS NCs. There are several reports on band-gap change by formation the nano-dots on the bulk. Facsko et al. [33] showed the blue-shift by formation of quantum dots on the GaSb bulk by Ar ion sputtering. Furthermore, Ar ion beam cleaning effect was investigated by Widodo and Terada [34] reporting the band-gap change of CIGS thin film after Ar ion beam etching was confirmed by photoemission spectroscopy and inverse photoemission spectroscopy. The surface with uniformly formed CIGS nano-dots would be a promising intermediate layer which has been considered as an important factor in enhancing optoelectronic and photovoltaic properties.

4. Conclusions

In this paper, we described the formation of self-organized CIGS nano-dots and nano-ridge structures on the surface of CIGS thin films under the normal incidence of an Ar ion beam. The ion beam irradiation duration and acceleration voltage were varied. At an irradiation time of 1 min and an ion beam acceleration voltage of 1 kV, nano-dots as small as 9 nm in diameter were formed. As the Ar ion irradiation time was increased, a shape transition from nano-dots to sharply etched nano-ridge structures occurred. The chemical composition of the CIGS NCs was changed such that a higher Cu content and a lower Se content were observed. However, as confirmed by the STEM/EDS and NBED analyses, the crystalline dots were found to have the same crystal structure as a pristine CIGS film. The formation mechanism and morphological evolution of the CIGS NCs can be understood on the basis of competition between the surface roughening by the ion beam sputtering and smoothing by surface diffusion in the multi-component system. From the low temperature PL measurements, the band-gap of the films increased from 1.06 for the pristine film to 1.16 eV for an Ar ion irradiated sample. This increase is due to the formation of nano-dots, which may be induced by a morphological effect. It is believed that this simple process for fabricating nano-dots on large area CIGS thin films will contribute to thin film solar cell performance.

Acknowledgments

We thank Prof. Kyung-suk Kim from Brown University for fruitful discussions. We acknowledge the financial support of grants from the R & D Program (2008-N-PV12-P-15) under the Korea Ministry of Knowledge Economy, Internal Project of KIST and the National Research Foundation of Korea (NRF) grants funded by the Korean Government (MEST) (Nos. 20110030803 and 20110019984).

References

[1] K.L. Chopra, P.D. Paulson, V. Dutta, Thin-film solar cells: an overview, Progress in Photovoltaics: Research and Application 12 (2004) 69–92.
[2] A. Chirila, S. Buecheler, F. Pianezzi, P. Bloesch, C. Gretener, A.R. Uhl, C. Fella, L. Kranz, J. Perrenoud, S. Seyrling, R. Verma, S. Nishiwaki, Y.E. Romanyuk, G. Bilger, A.N. Tiwari, Highly efficient Cu(In,Ga)Se_2 solar cells grown on flexible polymer films, Nature Materials 10 (2011) 857–861.
[3] M. Bär, I. Repins, MA. Contreras, L. Weinhardt, R. Noufi, C. Heske, Chemical and electronic surface structure of 20%-efficient Cu(In,Ga)Se_2 thin film solar cell absorbers, Applied Physics Letters 95 (2009) 052106-1–052106-3.
[4] P. Jackson, D. Hariskos, E. Lotter, S. Paetel, R. Wuerz, R. Menner, W. Wischmann, M. Powalla, New world record efficiency for Cu(In,Ga)Se_2 thin-film solar cells beyond 20%, Progress in Photovoltaics: Research and Application 19 (2011) 894–897.
[5] B. Li, Y. Xie, J.X. Huang, Y.T. Qian, Synthesis by a solvothermal route and characterization of $CuInSe_2$ nanowhiskers and nanoparticles, Advanced Materials 11 (1999) 1456–1459.
[6] Y. Jiang, Y. Wu, X. Mo, W.C. Yu, Y. Xied, Y.T. Qian, Elemental solvohermal reaction to produce ternary semiconductor $CuInE_2$ (E=S, Se) nanorods, Inorganic Chemistry 39 (2000) 2964–2965.
[7] Q.J. Guo, S.J. Kim, M. Kar, W.N. Shafarman, R.W. Birkmire, E.A. Stach, R. Agrawal, H.W. Hillhouse, Development of $CuInSe_2$ nanocrystal and nanoring inks for low cost solar cells, Nano Letters 8 (2008) 2982–2987.
[8] B. Koo, R.N. Patel, B.A. Korgel, Synthesis of $CuInSe_2$ nanocrystals with trigonal pyramidal shape, Journal of the American Chemical Society 131 (2009) 3134–3135.
[9] H. Peng, D.T. Schoen, S. Meister, X.F. Zhang, Y. Cui, Synthesis and phase transformation of In_2Se_3 and $CuInSe_2$ nanowires, Journal of the American Chemical Society 129 (2007) 34–35.
[10] S. Huang, Z. Dai, F. Qu, L. Zhang, X. Zhu, Self-assembled large-scale and cylindrical $CuInSe_2$ quantum dots on Indium Tin Oxide films, Nanotechnology 13 (2002) 691–694.
[11] S.Y. Huang, S. Xu, J.D. Long, Q.J. Cheng, X.B. Xu, J.B. Chu, Separated $CuInSe_2$ quantum dots on ZnO thin film by ICP-assisted magnetron sputtering, Surface Review and Letters 14 (2007) 225–228.
[12] D.T. Schoen, H.L. Peng, Y. Cui, Anisotropy of chemical transformation from In_2Se_3 to $CuInSe_2$ nanowires through solid state reaction, Journal of the American Chemical Society 131 (2009) 7973–7975.
[13] J. Xu, C.S. Lee, Y.B. Tang, X. Chen, Z.H. Chen, W.J. Zhang, S.T. Lee, W. Zhang, Z. Yang, Large-scale synthesis and phase transformation of CuSe, $CuInSe_2$, and $CuInSe_2$/$CuInS_2$ core/shell nanowire bundles, ACS Nano 4 (2010) 1845–1850.
[14] A. Niemegeers, M. Burgelman, R. Herberholz, U. Rau, D. Hariskos, H.-W. Schock, Model for electronic transport in Cu(In,Ga)Se_2 solar cells, Progress in Photovoltaics: Research and Application 6 (1998) 407–421.
[15] K.H. Kim, K.H. Yoon, J.H. Yun, B.T. Ahn, Effects of Se flux on the microstructure of Cu(In,Ga)Se_2 thin film deposited by a three-stage Co-evaporation process, Electrochemical and Solid-State Letters 9 (2006) A382–A385.
[16] D.J. Schroeder, G.D. Berry, A.A. Rockett, Gallium diffusion and diffusivity in $CuInSe_2$ epitaxial layers, Applied Physics Letters 69 (1996) 4068–4070.
[17] S. Facsko, H. Kurz, T. Dekorsy, Energy dependence of quantum dot formation by ion sputtering, Physical Review B 63 (2001) 165329-1–165329-5.
[18] A. Keller, A. Biermanns, G. Carbone, J. Grenzer, S. Facsko, O. Plantevin, R. Gago, T.H. Metzger, Transition from smoothing to roughening of ion-eroded GaSb surfaces, Applied Physics Letters 94 (2009) 193103-1–193103-3.
[19] R.Mark Bradley, James M.E. Harper, Theory of ripple topography induced by ion bombardment, Journal of Vacuum Science & Technology A 6 (1988) 2390–2395.
[20] V.B. Shenoy, W.L. Chan, E. Chason, Compositionally modulated ripples induced by sputtering of alloy surfaces, Physical Review Letters 98 (2007) 256101-1-4.
[21] The report of the National Physical Laboratory in UK. 〈http://www.npl.co.uk/science-technology/surface-and-nanoanalysis/services/sputter-yield-values〉.

[22] K. Gartsman, L. Chernyak, V. Lyahovitskaya, D. Cahen, V. Didik, V. Kozlovsky, R. Malkovich, E. Skoryatina, V. Usacheva, Direct evidence for diffusion and electromigration of Cu in $CuInSe_2$, Journal of Applied Physics 82 (1997) 4282–4286.
[23] T.D. Dzhafarov, M.S. Sadigov, E. Bacaksiz, D. Oren, I. Karabay, Effect of copper diffusion on photovoltaic characteristics of $CuGaSe_2$-GaAs cells, Solar Energy Materials & Solar Cells 52 (1998) 135–140.
[24] K. Djessas, A. Abatchou, G. Masse, Diffusions in (In,Se)–Cu(In,Ga)Se_2/SnO_2 thin film structure, Journal of Applied Physics 88 (2000) 5710–5715.
[25] D.J. Schroeder, G.D. Berry, A.A. Rockett, Gallium diffusion and diffusivity in $CuInSe_2$ epitaxial layers, Applied Physics Letters 69 (1996) 4068–4070.
[26] M. Marudachalam, R.W. Birkmire, H. Hichri, J.M. Schultz, A. Swartzlander, M.M. Al-Jassim, Phases, morphology, and diffusion in $CuIn_xGa_{1-x}Se_2$ thin films, Journal of Applied Physics 82 (1997) 2896–2905.
[27] X. Michalet, F.F. Pinaud, L.A. Bentolila, J.M. Tsay, S. Doose, J.J. Li, G. Sundaresan, A.M. Wu, S.S. Gambhir, S. Weiss, Quantum dots for live cells in vivo imaging, and diagnostics, Science 307 (2005) 538–544.
[28] A.P. Alivisatos, Semiconductor clusters, nanocrystals and quantum dots, Science 271 (1996) 933–937.
[29] Y. Yang, H. Lai, H. Xu, C. Tao, H. Yang, Morphology-luminescence correlations in europium-doped ZnO nanomaterials, Journal of Nanoparticle Research 12 (2010) 217–225.
[30] S. Shirakata, K. Ohkubo, Y. Lshii, T. Nakada, Effects of CdS buffer layers on photoluminescence properties of Cu(In,Ga)Se_2 solar cells, Solar Energy Materials & Solar Cells 93 (2009) 988–992.
[31] Y. Chiba, A. Yamada, M. Konagai, Y. Matsuo, T. Wada, Photoluminescence properties of Cu(InGa)Se_2 thin films prepared by mechanochemical process, Japanese Journal of Applied Physics 47 (2008) 694–696.
[32] T.R. Ravindran, A.K. Arora, B. Balamurugan, B.R. Mehta, Effects of Se flux on the microstructure of Cu(In,Ga)Se_2 thin film deposited by a three-stage co-evaporation process, Nanostructured Materials 11 (1999) 603–609.
[33] S. Facsko, T. Dekorsy, C. Koerdt, C. Trappe, H. Kurz, A. Vogt, H.L. Hartnagel, Formation of ordered nanoscale semiconductor dots by ion sputtering, Science 285 (1999) 1551–1553.
[34] Rusminto Tjatur Widodo, Norio Terada, Development of Ar ion beam etching treatment for surface cleaning of Cu($In_{1-x}Ga_x$)Se_2 [CIGS] thin films, Jurnal Nanosains & Nanoteknologi 3 (2010) 1–5.